Streptavidin-hydrogel prepared by sortase A-assisted click chemistry for enzyme immobilization on an electrode

Matsumoto, Takuya
Isogawa, Yuki
Tanaka, Tsutomu
Kondo, Akihiko

(Citation)
Biosensors & Bioelectronics,99:56-61

(Issue Date)
2018-01-15

(Resource Type)
journal article

(Version)
Accepted Manuscript

(URL)
https://hdl.handle.net/20.500.14094/90004620

Streptavidin-hydrogel prepared by sortase A-assisted click chemistry for enzyme immobilization on an electrode

Takuya Matsumoto,[†] Yuki Isogawa,[‡] Tsutomu Tanaka,[‡,] and Akihiko Kondo[†,‡]*

[†]Graduate School of Science, Technology and Innovation, Kobe University, 1-1 Rokkodaicho, Nada, Kobe 657-8501, Japan

[‡]Department of Chemical Science and Engineering, Graduate School of Engineering, Kobe University, 1-1 Rokkodaicho, Nada, Kobe 657-8501, Japan

[*]Corresponding author;

email: tanaka@kitty.kobe-u.ac.jp

tel:+81-78-803-6202

ABSTRACT

A tetrameric streptavidin (SA)-appended LPETG tag was site-specifically linked to azido-containing tri-glycine via sortase A catalysis and the resulting azido-modified SA (SA-N3) was retained in the biotin-binding pocket. SA-N3 was polymerized with dibenzylcyclooctyne-modified branched poly(ethyleneglycol) (DBCO-PEG) using azido-modified branched PEG (N3-PEG) as a spacer via copper-free click chemistry. The resulting SA-based hydrogel exhibited gel-like mechanical properties and could immobilize biotin-modified molecules through biotin-SA affinity. Glucose dehydrogenase (GDH) was immobilized in the SA-based hydrogel, and the hydrogel was then coated on a glassy carbon electrode (GCE) and used for the biocatalytic oxidation of glucose. The designed GCE exhibited better performance and stability compared with GDH chemically adsorbed onto a GCE. In addition, the designed GCE anode and a Pt-carbon cathode were assembled into a glucose/O_2 fuel cell that provided a maximum power density and open circuit voltage of 11.8 ± 0.56 μW cm^{-2} and 0.17 V, respectively.

Keywords: sortase A, streptavidin, hydrogel, bioanode

1. Introduction

Enzyme immobilization is an important technology for various biological systems and applications, including industrial and analytical applications (Ansari and Husain, 2012; DiCosimo et al., 2013), and for the generation of protein microarrays (Wong et al., 2009), biosensors, and biofuel cells (Willner et al., 2009; Rasmussen et al., 2016; Wang et al., 2016a). There has been significant research on methods for immobilizing enzymes on material surfaces, including crosslinking, adsorption, and entrapment (Ansari and Husain, 2012; DiCosimo et al., 2013; Homaei et al., 2013). Enzyme entrapment in hydrogels is one of the important approaches that retains the activity and conformation of the enzyme in a physiological environment (Kojuharova et al., 1988; Shiroya et al., 1995; Kim et al., 2011). Biomaterials such as chitosan and hyaluronic acid (Tang et al., 2014; Sun et al., 2015), or chemical materials such as poly(ethyleneglycol) (PEG) (Bayramoglu and Arica, 2014), are often used to provide a hydrogel base. The capacity of these materials for immobilized enzymes is increased by crosslinking, co-polymerization, or functionalization (Bayramoglu and Arica, 2014; Tang et al., 2014; Sun et al., 2015). However, an immobilized enzyme in a hydrogel is prone to leaking out of the gel because the enzyme is typically simply encapsulated within the small pores of the gel. Functional hydrogels that address this issue have recently been demonstrated and use functional building blocks such as protein (Guan et al., 2013; Kim et al., 2013; Ramirez et al., 2013). For example, a multimeric protein was used as a bridge site in a hydrogel backbone in order to utilize the protein's function. The artificial protein hydrogels use the trimeric protein CutA as a cross-linker. CutA and a self-assembling polypeptide co-polymer were mixed and formed a hydrogel that exhibited high stability in solutions at a wide range of pH values and temperatures (Guan et al., 2013; Ramirez et al., 2013). In addition, these protein hydrogels contain a motif for immobilizing

53 enzymes and are therefore used as a scaffold for immobilizing enzymes. Another approach
54 involves direct self-assembly and hydrogelation using three self-assembling multimeric
55 dehydrogenases that form a hydrogel that, coated on an electrode, is useful in enzymatic
56 methanol fuel cells (Kim et al., 2013). An alpha-helical leucine zipper domain and a random
57 structure soluble peptide domain were genetically introduced into each dehydrogenase to
58 promote heteromolecular self-assembly. The hydrogel-coated electrodes in the fuel cells
59 provided power and current densities comparable to those previously reported for similar enzyme
60 cascade systems (Palomre et al., 1998). These kinds of protein hydrogel retain high activity due
61 to encapsulation of the enzyme by self-assembling blocks and protein blocks that act as a
62 scaffold to immobilize the enzyme. An alternative approach is hydrogels constructed by direct
63 self-assembly of the enzyme of interest.

64 Here, we demonstrate a streptavidin (SA)-based hydrogel inspired by the former
65 strategy. SA is a tetrameric protein and is used as a bridge site in the hydrogel backbone. In
66 addition, SA has four biotin-binding pockets that can be used to immobilize other molecules,
67 including enzymes of interest (Green, 1990). We therefore anticipated that SA would be the ideal
68 protein building block for constructing a protein hydrogel as it would act both as a bridge site
69 and an immobilization site. Four-branched PEG was chosen to form the backbone of the
70 SA-hydrogel. Biotin-binding by SA was retained by using a methodology for self-assembling SA
71 and PEG without disrupting the biotin-binding pockets of SA: specifically, sortase A
72 (SrtA)-mediated protein ligation, and a bio-orthogonal chemical reaction for self-assembling SA
73 and PEG. Sortase A from *Staphylococcus aureus* is a transpeptidase that sorts enzymes for
74 displaying secreted proteins on the cell surface (Mazmanian et al., 1999). SrtA recognizes the
75 C-terminal LPXTG motif of a protein, and subsequently links a glycine oligomer to the

C-terminus through a native peptide bond. This ligation reaction has been used to prepare a variety of bioconjugates (Mao et al., 2004), to immobilize proteins (Ito et al, 2010; Hata et al., 2015), and to image cells (Tanaka et al., 2008). Although SrtA-mediated ligation is an attractive approach for tethering two different molecules, active SrtA is typically retained within the system after the SrtA-mediated reaction, thus requiring another step to remove SrtA (Witte et al., 2015). This complication can be addressed by combining SrtA-mediated ligation with bio-orthogonal cross-linking. To avoid the need for an extra step, target proteins are pre-modified with the bio-orthogonal group using SrtA-mediated site-specific ligation (Haridas et al, 2014). Click chemistry is a versatile bio-orthogonal reaction involving a cycloaddition between an azido group and a terminal alkyne (Beranardin et al., 2010). Click handles can be site-specifically incorporated into target molecules using site-specific SrtA-mediated ligation (Witte et al., 2013; Haridas et al., 2014; Wang et al., 2016b).

Herein, we prepared a SA-based hydrogel by SrtA-mediated click ligation. SA with a genetically-appended LPETG tag (SA-LP) was site-specifically tethered to an azido-GGG peptide using sortase A. The resulting azido-modified SA (SA-N3) was self-assembled with dibenzylcyclooctyne-modified branched PEG (DBCO-PEG) and azido-modified branched PEG (N3-PEG) as a spacer via copper-free click chemistry. The resulting SA-based hydrogel exhibited gel-like mechanical properties and could immobilize biotin-modified molecules through biotin-SA affinity. Here, the application of this hydrogel was demonstrated by immobilizing enzyme in the SA-based hydrogel, then coating this gel on a glassy carbon electrode (GCE). GDH was chosen as a model of immobilizing enzyme, which has been utilized for constructing glucose fuel cell (Willner et al., 2009). The prepared GCE exhibited biocatalytic

activity (glucose oxidation). This SA-based hydrogel provides a new way of immobilizing an enzyme of interest on a bioelectrode, and will also be useful for other biological applications.

2. Materials and methods

2.1. Materials. Four-branched PEG SUNBRIGHT PTE-200PA (MW 20,000 Da) was purchased from YUKA SANGYO CO., LTD. (Tokyo, Japan). Dibenzylcyclooctyne (DBCO)-Fluor545 was purchased from Funakoshi Co., Ltd. (Tokyo, Japan). N3-NHS-Ester (azido-dPEG$_4$-*N*-Succinimidyl Ester ester) was purchased from QUANTA BIODESIGN, LTD. (Montgomery, AL, USA). DBCO-NHS-Ester was purchased from Jena Bioscience GmbH (Thüringen, Germany). EZ-Link Sulfo-NHS-LC biotin was purchased from Thermo Fisher Scientific Inc. (Kanagawa, Japan). H-GGG-K(N3)-OH*HCl was purchased from Iris Biotech GmbH (Marktredwitz, Germany). PQQ-dependent glucose dehydrogenase was purchased from Toyobo Co., Ltd. (Osaka, Japan). KOD FX DNA polymerase, pCold IV vector, TALON metal affinity resin, a BCA protein assay kit, and *Escherichia coli* BL21(DE3) strain were purchased from Takara Bio Inc. (Shiga, Japan). All other chemicals were purchased from Nacalai Tesque (Kyoto, Japan).

2.2. Protein expression and purification. KOD FX DNA polymerase was used for the polymerase chain reaction (PCR). The gene encoding SA-LP was obtained by PCR using pColdI-SA-LPETG (Matsumoto et al., 2011) as the template with 5'-AGGTAATACCATATGATGAATCACAAAGTGCATCATCATCATCATCATGCCGAGGCC GGCATCACCGGC -3' as the 5' primer and 5'-ATTTACCTATCTAGACTAGCCGCCTGTTTCTGGCAAGGAGGCGGCGGACGGCTTC

AC-3' as the 3' primer. The amplified fragment was sub-cloned into the *NdeI*/*XbaI* sites of the pCold IV vector to yield pCold IV-SA-LP, which was then introduced into *Escherichia coli* BL21 (DE3). Cells were grown in Luria-Bertani medium at 37°C to an optical density (OD; 600 nm) of 0.5, and then the cells were incubated for an additional 30 min at 15°C. Protein expression was induced by the addition of isopropyl-β-D-thiogalactopyranoside to a final concentration of 0.5 mM. After growth for an additional 24 h at 15°C, the cells were harvested by centrifugation. The cell pellets were resuspended in 20 mM phosphate buffer (pH 8.0) containing 150 mM NaCl and then lysed using sonication. SA-LP was purified from the soluble fraction using TALON metal affinity resin according to the manufacturer's protocol and then dialyzed against 10 mM Tris-HCl buffer (pH 8.0) containing 150 mM NaCl. Additionally, His_6 tag appended SrtA (His_6-SrtA) was expressed and purified according to a previous report (Matsumoto et al., 2011). The concentration of purified proteins was determined using a BCA protein assay kit.

2.3. Preparation of azido-modified streptavidin. The modification reaction was performed in 50 mM Tris‑HCl, 150 mM NaCl, 10 mM $CaCl_2$, containing 0.003 mM His_6-SrtA, 0.03 mM Stav-LPETG, and 0.6 mM H-GGG-K(N3)-OH*HCl for 2 h at 37□ (pH 7.5, up to 600 μL). The unreacted H-GGG-K(N3)-OH*HCl and His_6-SrtA were removed by centrifugation in a viva spin 30K unit (30 kDa molecular weight cutoff). To verify the introduction of the azido group, the resulting SA-N3 solution was reacted with DBCO-Fluor545 (2 mM, 1 μL). The mixture was then mixed with Sodium dodecyl sulfate-Poly-Acrylamide Gel Electrophoresis (SDS-PAGE) sample buffer (50 mM Tris–HCl, 2% SDS, 6% 2-mercaptoethanol) and the samples were subjected to SDS-PAGE. The gels were stained with Coomassie brilliant blue R-250 (CBB) or analyzed using an LAS imager.

2.4. Construction of streptavidin-based hydrogel. The azido or DBCO group was modified with PEG by reacting N3-NHS or DBCO-NHS with four-branched amino-PEGs. Four-branched amino-PEG had four amino groups on termini, and amino-reacting NHS group was utilized for introducing N3 group or DBCO group in four termini of four-branched amino-PEG. SA-N3 solution (32 μM, 100 μL), N3-PEG (167 mg mL^{-1}, 30 μL) and DBCO-PEG (167 mg mL^{-1}, 30 μL) were mixed for one hour at RT to form the hydrogel. Rheometer measurements were performed using a Paar-Physica MCR-301 parallel plate rheometer (Anton Paar, Ashland, VA, USA) with a 25 mm plate fixture (PP25).

2.5. Preparation of the bioanode and biofuel cell. Biotinylated GDH was prepared by mixing PQQ-GDH (80 μM) and NHS-biotin (400 μM) for 2 hours at RT. Unreacted NHS-biotin was removed by centrifugation using a viva spin 30K unit, then the SA-N3 solution and the biotinylated (or non-biotinylated) GDH (two times of the stoichiometric molar equivalence of SA-N3) were added and mixed for 1 hour at RT. Here, the biotinylated (or non-biorinylated) GDH was attached to SA-N3 before forming a hydrogel in order to immobilize GDH in a hydrogel as well as on a hydrogel. The resulting GDH-SA-N3 (27 μL), N3-PEG (167 mg mL^{-1}, 1.25 μL) and DBCO-PEG (167 mg mL^{-1}, 1.25 μL) were dropped on a GCE surface (3 mm diameter, BAS Inc., Tokyo, Japan), that had been polished with alumina slurry. The electrode was allowed to dry for 90 min at RT (Scheme 1). Chemically GDH-immobilized GCE was prepared as follows. The GCE surface was modified by dropping non-biotynlated GDH solution (48 μM, 27 μL) and allowed to dry at RT. Poly-allylamine solution (5 μL, 1 wt.%) and glutaraldehyde (1 μL, 0.5 wt.%) were mixed on the GCE surface and allowed to dry overnight at RT. All prepared electrodes were stored at 4°C.

2.6. Electrochemical measurements. Electrochemical measurements were performed using a Model 2323 Bi-Potentiostat (BAS Inc.) and a conventional three-electrode cell. An Ag/AgCl electrode, a Pt wire, and prepared bioanodes were used as the reference electrode, counter electrode, and working electrode, respectively. Cyclic voltammetry (CV) was used to characterize the electrocatalytic properties of the bioanode with respect to glucose oxidation, and CV curves between –0.2 and +0.45 V were measured. Analysis of the open circuit voltage (OCV) was used to measure the electromotive force of the cells over a period of 10 s. Linear sweep voltammetry (LSV) was used to measure the maximum power density of the cells. All electrochemical measurements were conducted at room temperature and physiological pH.

3. Results and discussion

3.1. Sortase A-mediated click handle attachment onto streptavidin. The expression of recombinant SA usually requires a complex refolding process to reconstitute SA in an active form. We previously found that SA is expressed by a cold shock system without the formation of inclusion bodies (Matsumoto et al., 2011). Therefore, recombinant SA with the LPETG sequence attached at its C-terminus (SA-LP) was expressed using a cold shock system and purified with a His-tag affinity column. As shown in Figure 1A, triglycyl-ε-azido-L-lysine was then site-specifically tethered to the C-terminal LPETG sequence by SrtA-mediated ligation. The presence of the azido group was verified by mixing the resulting SA-N3 and DBCO-Fluor545. SA-N3 and DBCO-Fluor545 were linked by click reaction and the mixture was analyzed by SDS-PAGE. Figure 1B shows the stained gel and the LAS image after SDS-PAGE analysis. The band at around 60 kDa (corresponding to the molecular weight of SA) was only observed in lane

187 3, containing the SrtA-treated mixture. This result shows that SA-LP was successfully modified
188 at its C-terminus with the azido group using SrtA-mediated ligation.

189 **3.2. Hydrogelation of streptavidin triggered by click chemistry.** A hydrogel was formed
190 using SA-N3 by mixing branched PEG-appended click handles. The DBCO group at the
191 terminus of PEG was modified by mixing NHS-DBCO and one of four different branched PEGs
192 (linear: MW=10,000 and 20,000; Four-branched: MW=10,000 and 20,000), then the prepared
193 DBCO-PEGs were separately mixed with SA-N3. None of the mixtures formed hydrogels,
194 probably due to the exclusion of water molecules in the SA-PEG network (data not shown). To
195 address this, azido-PEG (N3-PEG) was added to the mixtures as a spacer. Only the mixture of
196 SA-N3 and DBCO-four-branched PEG (MW=20,000) effectively formed a hydrogel.
197 Rheological analysis confirmed that this hydrogel-like mixture was indeed a hydrogel. In
198 addition, the hydrogel showed a greater plateaued storage modulus (G') relative to the loss
199 modulus (G") over a wide range of strains or frequency (Figure 2A and 2B), verifying that the
200 gel-like mixture formed a hydrogel containing SA over a wide range of strains (Ramirez et al.,
201 2013).

202 **3.3. Biocatalytic glucose oxidation using a hydrogel-coated electrode.** An application of
203 the prepared SA-based hydrogel was demonstrated by immobilizing GDH on the hydrogel and
204 coating the mixture on a GCE (Scheme 1). GDH immobilized electrodes have been used in
205 glucose biosensors and glucose biofuel cells (D'Costa et al., 1986; Willner et al., 2009). GDH
206 oxidizes glucose to gluconolactone (gluconate), and small electron transferring molecules act as
207 a mediator to deliver an electron from glucose to the electrode (Mano et al., 2003). The
208 construction of this system requires that GDH be immobilized on an electrode in a highly active
209 and stable form. Direct immobilization, such as physical adsorption and chemical crosslinking,

often disrupts the conformation of an enzyme because the electrode surface is hydrophobic (Matsumoto et al., 2013; Tamaki et al., 2014). This can be addressed by, for example, coating the electrode with a hydrogel prior to immobilizing the enzyme (Alkasrawi et al., 1999). The prepared SA-based hydrogel can immobilize biotinylated enzymes; therefore, biotinylated GDH was immobilized in the SA-based hydrogel and the resulting GDH-SA-based hydrogel was coated on a GCE (Figure 3B; GS-GCE). Figure 3B shows the CV scan of glucose oxidation using the GS-GCE, demonstrating catalytic oxidation by the GS-GCE. In contrast, no catalytic oxidative current was observed using a SA-hydrogel-coated electrode (Figure 3A) containing entrapped non-biotinylated GDH (nGS-GCE), suggesting that insufficient GDH was retained in the SA-PEG hydrogel to measurably oxidize glucose. We then optimized the amount of immobilized GDH in SA-based hydrogels. The pore size of the SA-hydrogel was sufficient larger to hold active GDH because the network of the SA-hydrogel was composed of relatively longer PEG chains (20,000 kDa). In addition, sufficient amount of FC-COOH was added in a three-electrode system, hence the electronic communication was efficiently occurred between active embedded GDH in SA-hydrogel and the GC electrode. Hence we hypothesized that the increases of the amount of immobilized SA-GDH would facilitate the oxidation of glucose on the bioanode. As expected, the catalytic oxidative current in the presence of glucose was increased in the case that a ratio SA-GDH to PEG was 0.05 compared with the ratio was 0.04 or 0.02 (Figure 4A). However, the catalytic oxidative current was no longer increased in the case that the ratio was 0.1. This problem was probably due to the limited usable area on the electrode for effective electrical contact rather than the activity of embedded GDH in hydrogel. Therefore the optimum ratio of SA-GDH to PEG was as 0.05 in the current study and its stability and performance were evaluated. Next, we determined the stability of the hydrogel on the GCE in comparison with a

GCE coated with GDH chemically cross-linked using glutaraldehyde (1 μL, 0.5 wt.%) and poly-arylamimne (5 μL, 1 wt.%) (GC-GCE) (Matsumoto et al., 2013). Although an equal amount of GDH was immobilized on the GCE by both methods, the GS-GCE retained high catalytic activity of GDH compared to the GC-GCE after 4 days of cycling (Figure 4), demonstrating that the prepared SA-based hydrogel is superior for immobilizing enzymes in their stable and active form on a GCE compared to chemical crosslinking. However, the catalytic activity of GS-GCE clearly decreased after a week of cycling (data not shown), and the stability of the GS-GCE was not competent compared with enzyme electrodes with other reports (Mizutani et al., 1998; Chen et al., 2011; Korani et al., 2013), maybe because simple adsorption of SA-hydrogel on GCE leaded to peeling of SA-hydrogel on GCE after long time incubation. Therefore further investigation to hold SA-hydrogel on GCE is required, including layer-by-layer method (Mizutani et al., 1998) and combination with chitosan- or silk-film (Chen et al., 2011; Liu et al., 2012).

3.4. Assembly of a glucose/O_2 fuel cell. A two-compartment glucose/O_2 fuel cell (GFC) was constructed using a GS-GCE as the bioanode and a Pt-carbon-adsorbed GCE as the cathode to provide a GS-GFC (Figure 5 (A)). The fuel cell was assembled by immersing the bioanode in 100 mM phosphate buffer (pH 7.0) containing 20 mM glucose and 2.0 mM Fc-COOH and the cathode in 100 mM phosphate buffer (pH 7.0) containing 7.4 mM sulfate sodium. The two compartments were separated by a Nafion membrane. Figure 5 (B) shows the current and power density of the assembled GFC as a function of operating cell voltage (I–V and P–V curves) at RT. The maximum power density of the assembled GS-GFC was 11.8 ± 0.56 μW cm^{-2} (10.95 μW cm^{-2} at 0.17 V in Figure 5 (B)). The performance (maximum power density) of this GFC was somewhat lower than that of other GFCs previously reported due to the use of electrodes with

small surface areas or insufficient electrochemical communication with non-immobilized FC-COOH as a mediator. Tanne et al has employed multi-walled carbon nanotubes to improve the electrochemical communication between GDH and electrode, and the fuel cell exhibited maximal power density of about 23 μW cm^{-2} (Tanne et al., 2010). Also, Scherbahn et al has used two different types of carbon nanotube as interface. The buckypaper-based fuel cells exhibited maximal power density of about 107 μW cm^{-2} and the vertically aligned carbon nanotubes-based fuel cell achieves a maximal power density of 122 μWcm^{-2} (Scherbahn et al., 2014). Thus, further investigations, including the use of large surface area electrodes allowing the use of a large amount of enzyme and the improvement of electrochemical communication between enzyme and electrode, may improve the performance of the GFC.

4. Conclusions

In summary, we have prepared a new hydrogel composed of tetrameric SA and branched PEG. SA was used as a bridge site in the hydrogel backbone to provide a new platform for immobilizing enzymes in the hydrogel. The utility of this approach was demonstrated by using this SA-based hydrogel as a scaffold to immobilize highly active and stable enzyme on an electrode. SA-based hydrogel is a promising new approach for enzyme immobilization and other applications such as drug delivery and tissue engineering.

ACKNOWLEDGMENTS

This work was supported by Special Coordination Funds for Promoting Science and Technology, provided by the Creation of Innovation Centers for Advanced Interdisciplinary Research Areas

277 (Innovative Bioproduction Kobe), MEXT, Japan. We thank Dr. Yoshiyuki Komoda for use and
278 technical assistance with a Paar-Physica MCR-301 parallel plate rheometer.

279

REFERENCES

Alkasrawi, M., Popescu, I.C., Laurinavicius, V., Mattiassona, B., Csöregi, E., 1999, Anal. Commun. 36, 395–398

Ansari, S.A, Husain, Q., 2012. Biotechnol. Adv. 30, 512-513.

Bayramoglu, G., Arica, M.Y., 2014. Bioprocess Biosyst. Eng. 37, 235-243.

Bernardin, A., Cazet, A., Guyon, L., Delannoy, P., Vinet, F., Bonnaffé, D., Texier, I., 2010. Bioconjug. Chem. 21, 583-588.

Chen, C., Wang, L., Tan, Y., Qin, C., Xie, F., Fu, Y., Xie, Q., Chen, J., Yao, S., 2011. Biosens. Bioelectron. 26, 2311-2316.

D'Costa, E.J., Higgins, I.J., Turner, A.P.F., 1986. Biosensors 2, 71-87.

DiCosimo, R., McAuliffe, J., Poulose, A.J., Bohlmann, G., 2013. Chem. Soc. Rev. 42, 6437-6474.

Green, N.M., 1990. Methods Enzymol. 184, 51-67.

Guan, D., Ramirez, M., Shao, L., Jacobsen, D., Barrera, I., Lutkenhaus, J., Chen, Z., 2013. Biomacromolecules 14, 2909-2916.

Haridas, V., Sadanandan, S., Dheepthi, N.U., 2014. Chembiochem 15, 1857-1867.

Hata, Y., Matsumoto, T., Tanaka, T., Kondo, A., 2015. Macromol. Biosci. 15, 1375-1380.

Homaei, A.A., Sariri, R., Vianello, F., Stevanato, R., 2013. J. Chem. Biol. 6, 185-205.

298 Ito, T., Sadamoto, R., Naruchi, K., Togame, H., Takemoto, H., Kondo, H., Nishimura, S., 2010.
299 Biochemistry 49, 2604-2614.

300 Kim, J.H., Lim, S.Y., Nam, D.H., Ryu, J., Ku, S.H., Park, C.B., 2011. Biosens. Bioelectron. 26,
301 1860-1865.

302 Kim, Y.H., Campbell, E., Yu, J., Minteer, S.D., Banta, S., 2013. Angew. Chem. Int. Ed. Engl. 52,
303 1437-1440.

304 Kojuharova, A., Popova, Y., Kirova, N., Klissurski, D., Simeonov, D., Spasov, L., 1988. J. Chem.
305 Technol. Biotechnol. 42, 95–104.

306 Korani, A., Salimi, A., 2013. Biosens. Bioelectron. 50, 186-193.

307 Liu, J., Zhang, X., Pang, H., Liu, B., Zou, Q., Chen, J., 2012, Biosens. Bioelectron. 31, 170-175.

308 Mano, N., Mao, F., Heller, A., 2003. J. Am. Chem. Soc. 125, 6588-6594.

309 Matsumoto, T., Sawamoto, S., Sakamoto, T., Tanaka, T., Fukuda, H., Kondo, A., 2011. J.
310 Biotechnol. 152, 37-42.

311 Matsumoto, T., Shimada, S., Yamamoto, K., Tanaka, T., Kondo, A., 2013. Fuel Cells 13,
312 960-964.

313 Mao, H., Hart, S.A., Schink, A., Pollok, B.A., 2004. J. Am. Chem. Soc. 126, 2670-2671.

314 Mazmanian, S.K., Liu, G., Ton-That, H., Schneewind, O., 1999. Science 285, 760-763.

315 Mizutani, F., Sato, Y., Hirata, Y., Yabuki, S., 1998. Biosens. Bioelectron. 13, 809-815.

316 Palmore, G.T.R., Bertschy, H., Bergens, S.H., Whitesides, G.M., 1998. J. Electroanal. Chem.
317 443, 155-160.

318 Ramirez, M., Guan, D., Ugaz, V., Chen, Z., 2013. J. Am. Chem. Soc. 135, 5290-5293.

319 Rasmussen, M., Abdellaoui, S., Minteer, S.D., 2016. Biosens. Bioelectron. 76, 91-102.

320 Scherbahn, V., Putze, M.T., Dietzel, B., Heinlein, T., Schneider, J.J., Lisdat, F., 2014. Biosens.
321 Bioelectron. 61, 631-638.

322 Shiroya, T., Tamura, N., Yasui, M., Fujimoto, K., Kawaguchi, H., 1995. Colloids Surf. B
323 Biointerfaces. 4, 267-274.

324 Sun, H., Yang, H., Huang, W., Zhang, S., 2015. J. Colloid Interface Sci. 450, 353-360.

325 Tamaki, T., Sugiyama, T., Mizoe, M., Oshiba, Y., Yamaguchi, T., 2004. J. Electrochem. Soc., 16,
326 H3095-H3099.

327 Tanaka, T., Yamamoto, T., Tsukiji, S., Nagamune, T., 2008. Chembiochem 9, 802-807.

328 Tang, D.W., Yu, S.H., Wu, W.S., Hsieh, H.Y., Tsai, Y.C., Mi, F.L., 2014. Colloids Surf. B
329 Biointerfaces 113, 59-68.

330 Tanne, C., Göbel, G., Lisdat, F., 2010. Biosens. Bioelectron. 26, 530-535.

331 Wang, T., Hou, C., Zhang, Y., He, F., Liu, M., Lia, X., 2016a. J. Mater. Chem. B 4, 3695-3702.

332 Wang, L., Jiang, R., Wang, L., Liu, Y., Sun, X.L., 2016b. Bioorg. Chem. 65, 159-166.

333 Willner, I., Yan, Y.M., Willner, B., Tel-Vered, R., 2009. Fuel Cells 9, 7-24.

334 Witte, M.D., Theile, C.S., Wu, T., Guimaraes, C.P., Blom, A.E., Ploegh, H.L., 2013. Nat. Protoc.
335 8, 1808-1819.

336 Witte, M.D., Wu, T., Guimaraes, C.P., Theile, C.S., Blom, A.E., Ingram, J.R., Li, Z., Kundrat, L.,
337 Goldberg, S.D., Ploegh, H.L., 2015. Nat. Protoc. 10, 508-516.

338 Wong, L.S., Khan, F., Micklefield, J., 2009. Chem. Rev. 109, 4025-4053.

339

340 **Figure Captions**

341 **Scheme 1.** The schematic illustration of the preparation of enzyme-streptavidin based hydrogel

342 **Figure 1.** (A) Schematic illustration of SrtA-mediated click handle modification of the C-termini
343 of streptavidin (SA) and click reaction between N3-SA and DBCO-Fluor545. (B) SDS-PAGE
344 analysis of the reaction mixtures with NH2-GGGK(N3)-OH after processing with
345 DBCO-Fluor545. The CBB stained gel (left). LAS image (excitation: 488 nm, emission: 509 nm)
346 (right). Lane M: Dual color standard marker. Lane 1: SA-LP. Lane 2: SrtA. Lane 3: SA-LP and
347 SrtA.

348 **Figure 2.** Rheological characterization of SA-based hydrogel: (A) angular frequency sweep at
349 1% strain, (B) strain sweep at 10 rad s^{-1}, representing storage modulus with closed circle, and
350 loss modulus with open triangle.

351 **Figure 3.** CV of the nGS-GCE (A) and the GS-GCE (B) in 0.1 M phosphate buffer, pH 7.0
352 containing 2.0 mM Fc-COOH (blue line) and 20 mM glucose (red line). Data were collected at
353 10 mV s^{-1}.

Figure 4. (A) The influence of the amount of containing SA-GDH in hydrogels on catalytic oxidation of glucose; the current density of CV of the GS-GCE in 0.1 M phosphate buffer, pH 7.0 containing 2.0 mM Fc-COOH and 20 mM glucose. (B) Relative current density of the oxidative current peak at CV of the GS-GCE (red symbols) and GC-GCE (blue symbols) in 0.1 M phosphate buffer, pH 7.0, containing 2.0 mM Fc-COOH and 20 mM glucose. Error bars represent standard deviation.

Figure 5. (A) Schematic illustration of assembled fuel cell in this study. (B) Power density curve of the glucose/O_2 biofuel cell obtained by LSV using GS-GCE as the bioanode and a Pt-carbon-coated GCE as the cathode. Data were collected at 5 mV s^{-1}.

Scheme 1

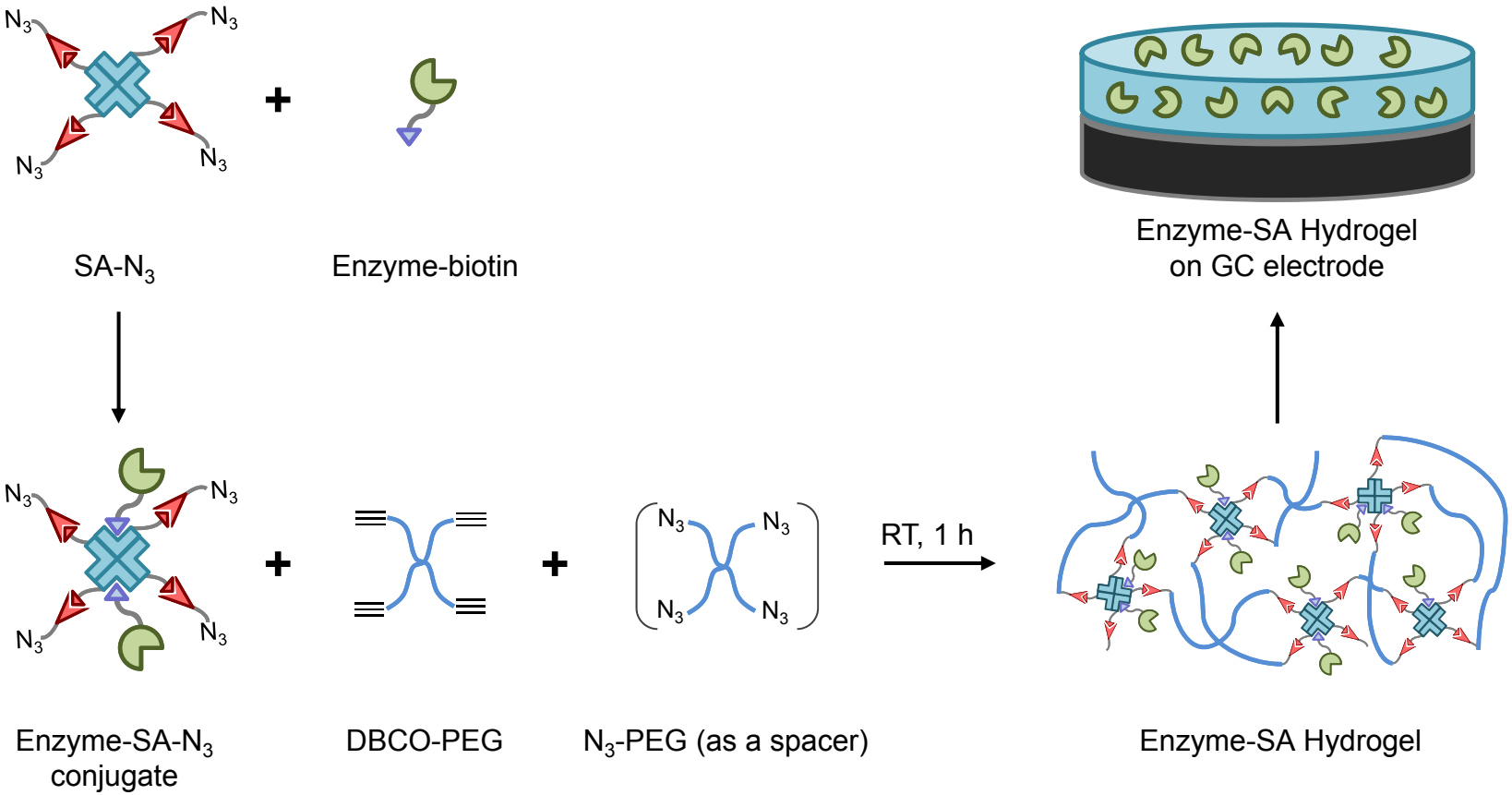
N3
N3
N3
N3
+
SA-N3
Enzyme-biotin
Enzyme-SA Hydrogel
on GC electrode
N3
N3
N3
N3
+
+
N3
N3
N3
N3
RT, 1 h
Enzyme-SA-N3
conjugate
DBCO-PEG
N3-PEG (as a spacer)
Enzyme-SA Hydrogel

Figure 1

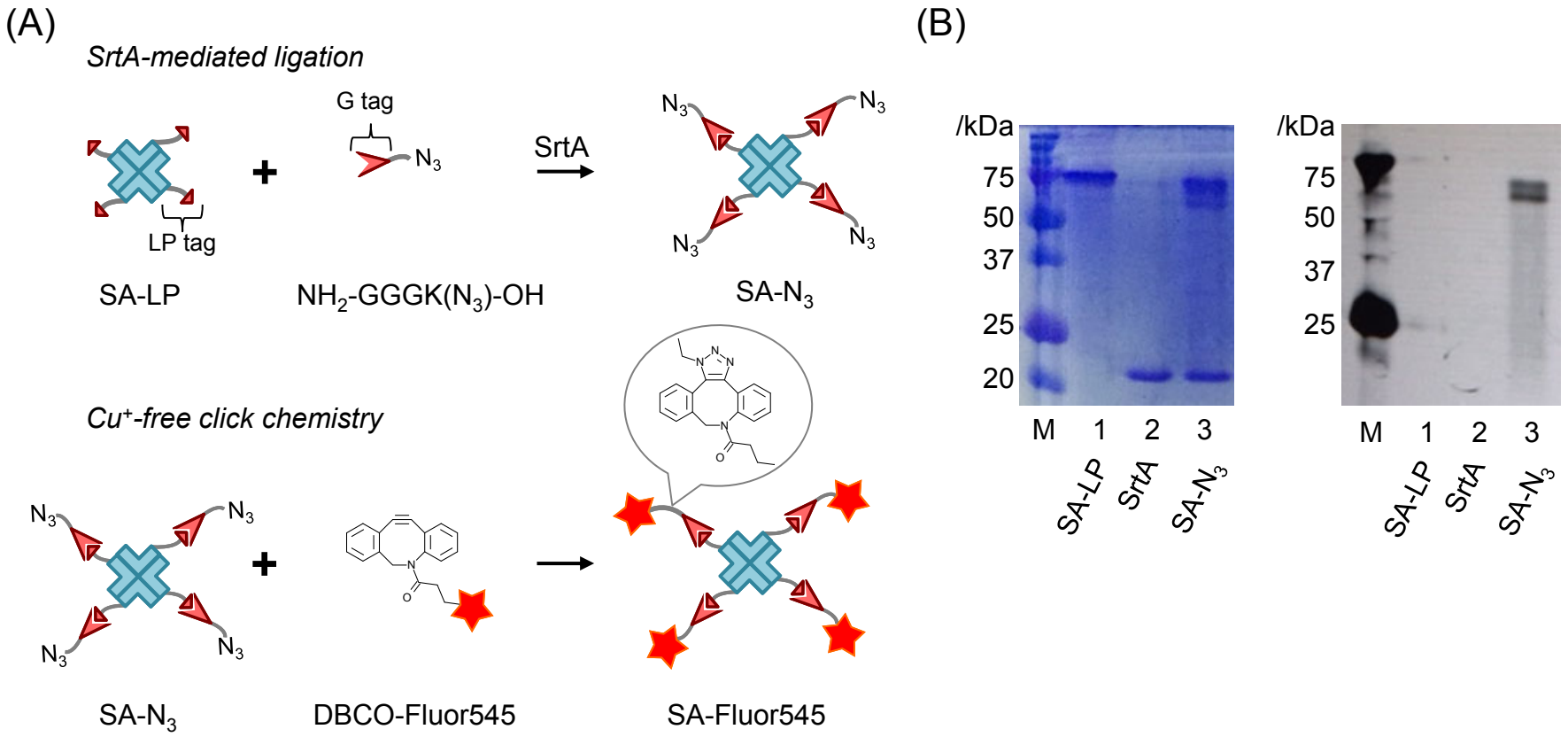
(A)
SrtA-mediated ligation
G tag
LP tag
SrtA
SA-LP
NH2-GGGK(N3)-OH
SA-N3
Cu+-free click chemistry
SA-N3
DBCO-Fluor545
SA-Fluor545
(B)
/kDa
75
50
37
25
20
M
1
2
3
SA-LP
SrtA
SA-N3

Figure 2

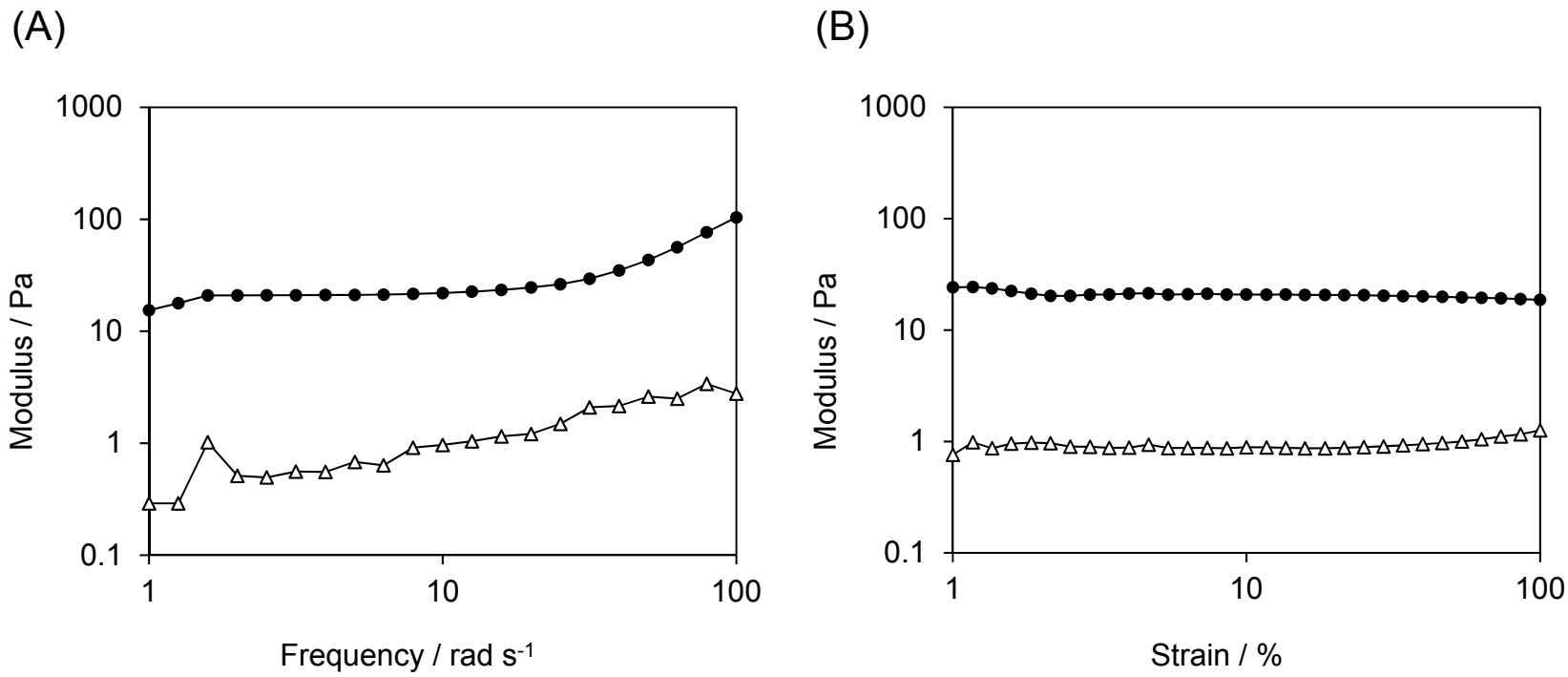
(A)
1000
100
10
1
0.1
Modulus / Pa
1
10
100
Frequency / rad s-1
(B)
1000
100
10
1
0.1
Modulus / Pa
1
10
100
Strain / %

Figure 3

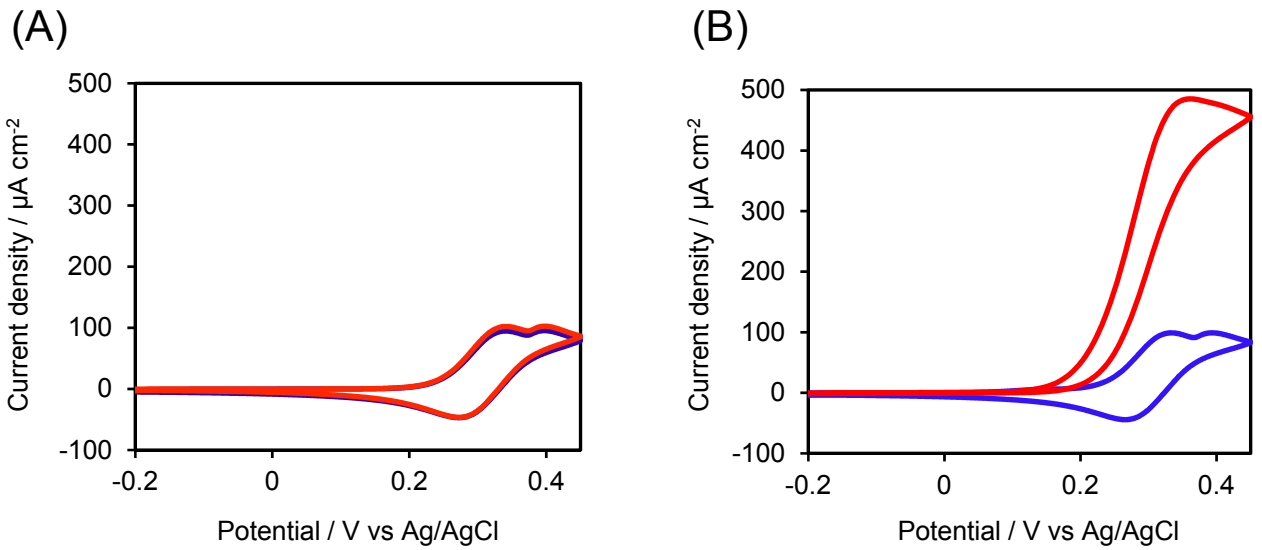
(A)
(B)
Current density / µA cm-2
500
400
300
200
100
0
-100
-0.2
0
0.2
0.4
Potential / V vs Ag/AgCl

Figure 4

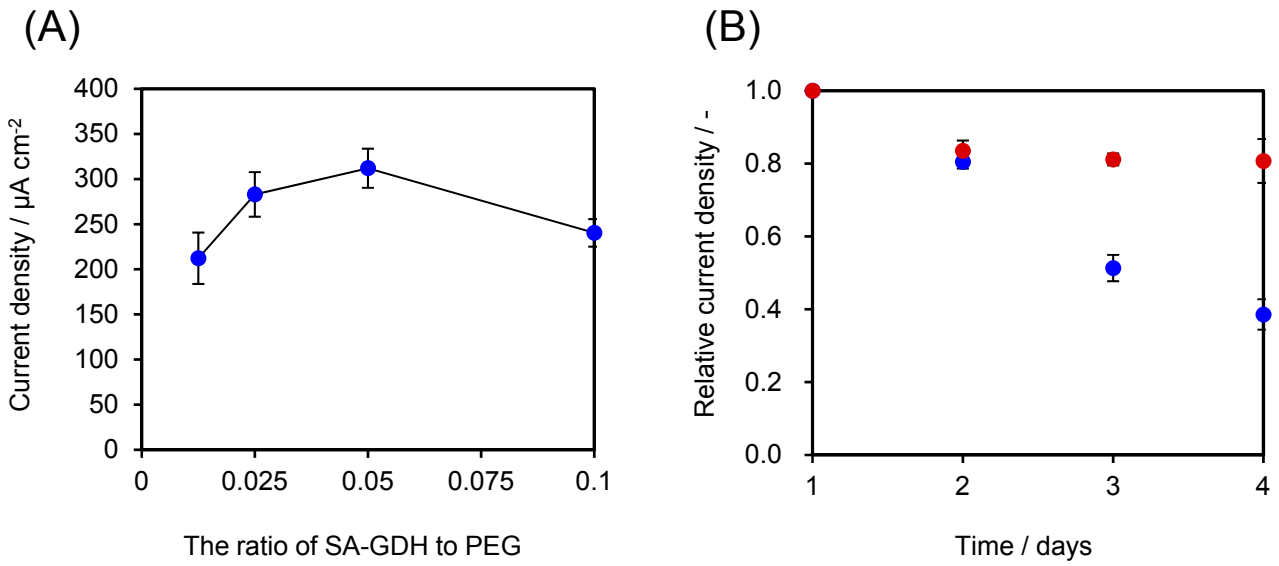
(A)
Current density / μA cm-2
400
350
300
250
200
150
100
50
0
0
0.025
0.05
0.075
0.1
The ratio of SA-GDH to PEG
(B)
Relative current density / -
1.0
0.8
0.6
0.4
0.2
0.0
1
2
3
4
Time / days

Figure 5

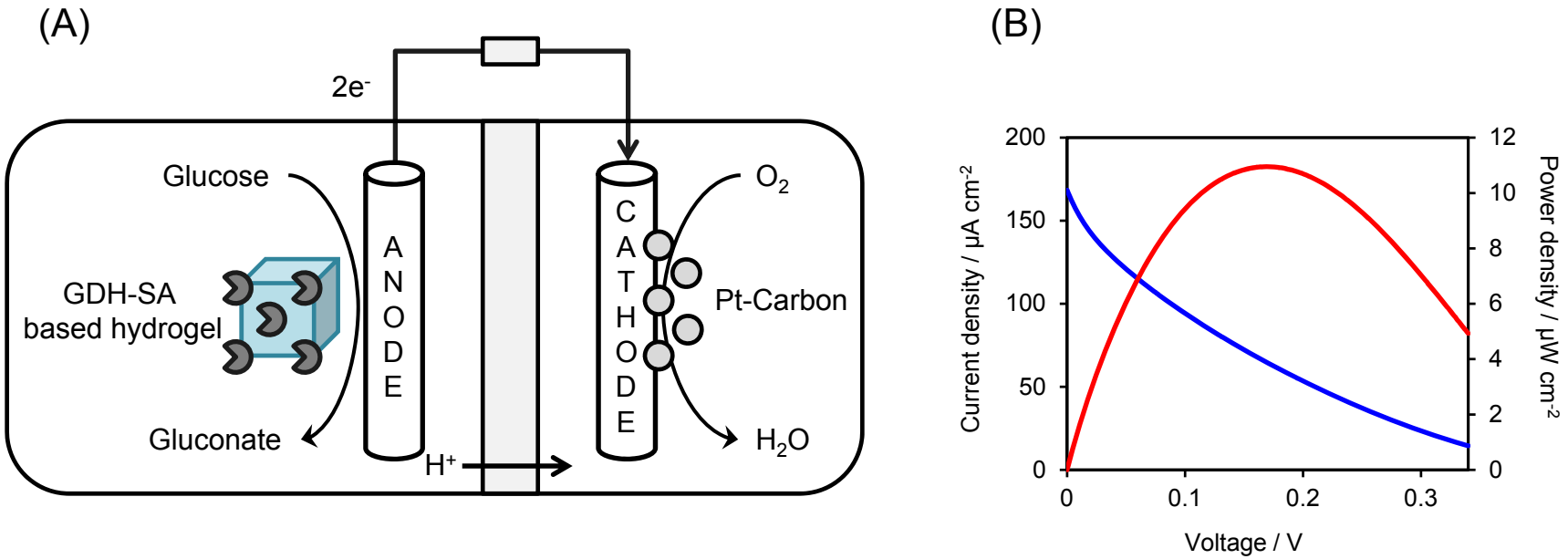
(A)
2e-
Glucose
GDH-SA
based hydrogel
Gluconate
ANODE
H+
CATHODE
O2
Pt-Carbon
H2O
(B)
Current density / μA cm-2
Power density / μW cm-2
Voltage / V
0
50
100
150
200
0
2
4
6
8
10
12
0
0.1
0.2
0.3